Dalton Transactions

Accepted Manuscript

ROYAL SOCIETY OF CHEMISTRY

www.rsc.org/dalton

Journal Name

RSCPublishing

ARTICLE

Proton conductive watery channels constructed by Anderson polyanions and lanthanide coordination cations

Cite this: DOI: 10.1039/xoxxoooooox

Received ooth January 2012,
Accepted ooth January 2012

DOI: 10.1039/xoxxoooooox

www.rsc.org/

Jun Miao,[a] Yiwei Liu,[a] Qun Tang,[a] Danfeng He,[a] Guocheng Yang,[b] Zhan Shi[c], Shuxia Liu[a*] and Qingyin Wu[d]

A 3D inorganic-organic hybrid proton conductor, $[Sm(H_2O)_5(CO_2CH_2NH_3)_2][Al(OH)_6Mo_6O_{18}]\cdot 10H_2O$ (**1**), has been synthesized by using coordination cations, $[Sm(H_2O)_5(gly)_2]^{3+}$ (gly = $^-CO_2CH_2NH_3^+$), and polyanions, $[Al(OH)_6Mo_6O_{18}]^{3-}$ ($[AlMo_6]$). The polyanions ($[AlMo_6]$) and the coordination cations ($[Sm(H_2O)_5(gly)_2]^{3+}$) stack to form a 3D supramolecular network structure containing 1D channels along c axis by electrostatic force and H-bonded interaction. Significantly, the 1D channels are water-filled with a high water content (both Sm coordinated and in lattice). Dynamic adsorption measurement was implemented at 1atm, 95% relative humidity (RH). The water adsorption amount (6.51 wt% at 25 °C and 5.68 wt% at 80 °C) consistent with the number of lattice water molecules of **1** suggests that water chains were retained at elevated temperatures (80 °C) under 95% RH. Alternating-current (AC) impedance measurements of **1** reveal an outstanding conductivity for **1** is 4.53×10^{-3} $S\cdot cm^{-1}$ at 80 °C under 95% RH. The activation energy of **1** calculated from Arrhenius plots of the proton conductivity is 1.09 eV, which indicated that the protons transfer by vehicle mechanism.

Introduction

Inspired by the application of proton conductor in fuel cells, many researchers are interested in developing solid proton-conducting materials with conductivity of 10^{-4} $S\cdot cm^{-1}$ or above.[1-4] Recently, much attention has been paid toward the syntheses of inorganic-organic hybrids for proton conduction.[5-9] In general, these materials require proton carriers given by acid or hydroxyl groups and proton-conducting pathways composed of hydrophilic channels or hydrogen-bond networks.[10, 11] Both a large amount and a high mobility of proton carriers are required to provide good proton conductivity.[12] The proton transport may occur through water molecules and hydroxonium ions which moved directionally in the pathway. Alternatively, protons may transfer between water molecules and hydroxonium ions through the hydrogen-bonded chains.[13-19]

Polyoxometalates (POMs) are a subset of anionic early transition-metal oxide clusters with unique physical and chemical properties.[20-23] The applications of these POMs have attracted considerable attention in catalysis, medicine, materials science, or nanotechnology.[24-27] Due to the fact that POMs have discrete and mobile ionic structures, these solids possess strong Brønsted acidity and "pseudoliquid phase" behaviour.[28, 29] It is worth noting that these properties in acid-base catalysis are generally correlated with proton conductivities of solids.[30, 31] Hence, POMs have been regarded as attractive candidates for proton conduction. In 1979, Nakamura first reported $H_3PM_{12}O_{40}\cdot 29H_2O$ (M = Mo, W) as a proton conductor.[32] Since then, developments on the conductivity of POMs have concentrated upon transition metal-substituted heteropolyacids (HPAs) and POM-MOFs.[30, 31, 33-39] In these compounds, the conductivity generally arises from guest water and coordinated water as proton donors or carriers; furthermore, it could also be caused by the characteristics of a "pseudoliquid phase" with high proton mobility. However, HPAs are water-soluble, and disfavor of determined proton transfer pathways limits their development in high proton conduction.

A couple of years ago, a large number of porous ionic crystals based on polyoxometalates and molecular cations (macrocations) were reported.[40-43] As transferable inorganic building blocks, POMs have been applied in the preparation of functional materials based on ionic networks.[38, 39, 43] Solubility and aggregation state of POM-based ionic crystals can be finely tuned by the choice of sizes, shapes, charges, and ligands of the constituent ions.[40] Polyanions and macrocations can form hydrophilic channels in the ionic crystals by strong electrostatic force which is suitable for accommodating guest molecules in crystal lattice.[43] Despite the promising advancement in channel-selective sorption,[40-43] there are still some challenges and opportunities to develop the porous ionic crystals for proton

conduction. Guest (water) molecules in the channels to form a facile proton conduction pathway make them potential candidates for proton-conducting materials. However, there have hitherto been rare reports of POM-based ionic crystals for proton conduction.[38, 39, 44-46]

In this work, an ionic network based on Anderson POM, $[Sm(H_2O)_5(CO_2CH_2NH_3)_2][Al(OH)_6Mo_6O_{18}]\cdot 10H_2O$ (**1**), was synthesized and characterized. The single crystal was obtained by slow crystallization at room temperature from acidic (pH ≈ 2.6) aqueous solutions. Single crystal X-ray diffraction analysis revealed that compound **1** is constructed by $[Sm(H_2O)_5(CO_2CH_2NH_3)_2]^{3+}$ and $[Al(OH)_6Mo_6O_{18}]^{3-}$ possessing a high water content (both Sm coordinated and in the lattice), and significantly, the other characteristic of **1** is the presence of repetitive array of water molecules in 1D channels. Both features are considered to be beneficial for proton conduction. The outstanding conductivity of 4.53×10^{-3} $S\cdot cm^{-1}$ for **1** was achieved at 80 °C under 95% RH. The effect of the glycine ligand on the conductivity properties was also investigated.

Experimental

Materials

All chemicals were used as purchased without further purification. Elemental analyses were performed on a Perkin–Elmer 240C elemental analyzer and a PLASMASPEC(I) ICP atomic emission spectrometer. IR spectra were recorded in the range 400–4000 cm^{-1} on an Alpha Centaurt FT/IR spectrophotometer using KBr pellets. TG analyses were performed on a Perkin–Elmer TGA7 instrument in flowing N_2 with a heating rate of 10°C /min. Powder X-ray diffraction measurements were performed on a Rigaku D/MAX-3 instrument with Cu KR radiation in the angular range 2θ = 5-50 ° at 293 K.

Synthesis of $[Sm(H_2O)_5(gly)_2][Al(OH)_6Mo_6O_{18}]\cdot 10H_2O$ and preparation of $La(H_2O)_7[Al(OH)_6Mo_6O_{18}]\cdot 4H_2O$

$[Sm(H_2O)_5(CO_2CH_2NH_3)_2][Al(OH)_6Mo_6O_{18}]\cdot 10H_2O$ (**1**) was synthesized using reported synthetic methods.[47]

$Na_2MoO_4\cdot 2H_2O$ (0.90 g, 3.7 mmol) was added to 15 mL acetic acid solution (volume ratio of water: acetic acid= 2:1). The mixture and a 30 mL aqueous solution of $AlCl_3\cdot 6H_2O$ (0.36 g, 1.5 mmol) was mixed. Then a 10 mL water solution of glycine (0.09 g, 1.2 mmol) and $SmCl_3\cdot 6H_2O$ (0.22 g, 0.6 mmol) was added. The pH of the resulting mixture was adjusted with dilute hydrochloric acid to about 2.6 and it was stirred for half an hour. A large amount of colorless block crystals formed after 4 hours collected in about 61% yield (based on Mo).

Elemental Anal. Calc. for $C_4H_{36}AlSmMo_6N_2O_{38}$: C, 3.26; H, 2.46; N, 1.90; Al, 1.83; Sm, 10.21; Mo, 39.07. Found: C, 3.22; H, 3.18; N, 1.96; Al, 1.61; Sm, 9.48; Mo, 36.44%. IR (KBr, cm^{-1}): 3384 (br), 1587 (m), 1555 (m), 1472 (s), 1423 (m), 1338 (m), 1111 (m), 952 (m), 890 (s), 650 (s), 582 (m), 446 (m).

Preparation method of $La(H_2O)_7[Al(OH)_6Mo_6O_{18}]\cdot 4H_2O$ is presented according to literature.[48]

Crystal Structure determination

The reflection intensity data of **1** was collected on a SMART CCD diffractometer equipped with graphite monochromatic Mo KR radiation (λ = 0.71073 Å) at 293 K. The linear absorption coefficients, scattering factors for the atoms, and anomalous dispersion corrections were taken from International Tables for X-ray Crystallography. The structure was solved by the direct method and refined by the full-matrix least squares method on F_2 using the SHELXTL crystallographic software package. All H atoms were placed geometrically for **1**. Anisotropic thermal parameter was used to refine all non-hydrogen atoms. Large Max. (Positive) Residual Density 4.84 eA^{-3} in the crystal structure is near Sm1 and O14 with a distance of 2.434 Å and 1.472 Å, respectively. Thus, it is not suitable to be assigned as any atoms, which can be interpreted as Fourier truncation errors. The crystal data and structure refinement results of compound **1** are summarized in Table 1.

Table 1 Crystal data and structure refinement parameters for **1**.

	1
Empirical formula	$C_4H_{45}AlMo_6N_2O_{43}Sm$
M	1562.37
Crystal system	Monoclinic
Space group	C2/c
θ Range (°)	3.44–26.00
a (Å)	33.101(13)
b (Å)	10.690(4)
c (Å)	11.876(4)
β (°)	106.485(8)
V ($Å^3$)	4029(3)
Z	4
F(000)	3016
D_c (g cm^{-3})	2.576
Absorption coefficient (mm^{-1})	3.389
Total data collected	16796
Unique data	3935
R_{int}	0.0530
Goodness-of-fit	1.143
R_1 [I > 2σ(I)][a]	0.0768
wR_2 [I > 2σ(I)][b]	0.2058

[a] $R_1 = \sum||F_0|-|F_c||/\sum|F_0|$.

[b] $wR_2 = [\sum w(F_0^2-F_c^2)^2/\sum w(F_0^2)^2]^{1/2}$.

Vapour sorption Measurements

The water sorption measurements were performed with Micromeritics ASAP 2020 surface area and porosity analyser and Hiden Isochema Intelligent Gravimetric Analyser (IGA-100B).

The sample (~100 mg) was outgassed to a constant weight at 90°C under a high vacuum (< 10^{-6} mbar) prior to measurement of the isotherms. The saturated vapour pressure of the sorbent (water) at 298 K is 31.8 mbar. High purity N_2 (99.999%) was used as carrier gas for the adsorption of H_2O. The total flow rate throughout the experiments was kept constant at 500 ± 1 cm^3 min^{-1}, while the pressure was maintained constant at 1000 ± 1 mbar and the temperature variation was < 0.1°C. The purge

process was performed by outgassing with the rate of 10 mbar min^{-1}. The temperatures of 298 K and 353 K were maintained constant-temperature water bath.

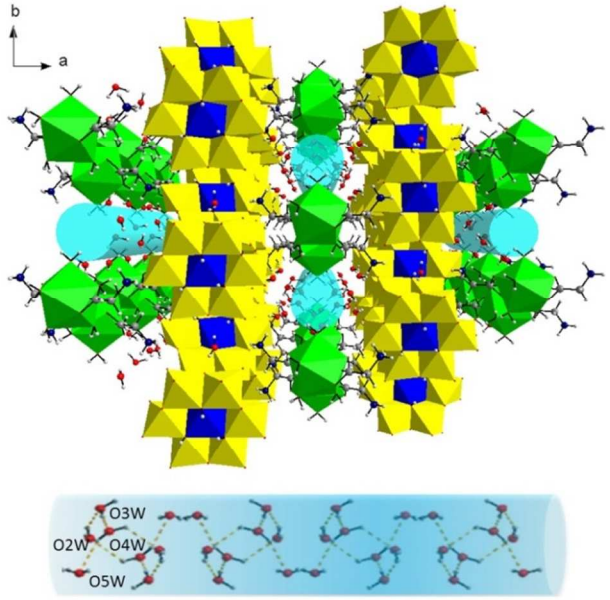

Fig. 1 Polyhedral representation of 3D supramolecular network structure containing 1D channel constructed by Anderson polyanions and samarium coordination cations.(top) Simplified schematic representation of water chains along 1D channels for **1**.(bottom) Colour code: Al, blue octahedron; Mo, yellow octahedron; Sm, green polyhedron; N, mazarine; C, grey; O, red; H, ashgrey.

Conductivity characterization

Impedance measurements of the products were performed on a PARSTAT 2273 (AMETEK Instruments, USA) electrochemical workstation. The product was compressed to a disc under a pressure of 30 MPa at room temperature. The diameter was 10 mm and the thickness was 3.8 mm. Two copper sheets were attached to the faces of the disc. Copper slices and copper wires were used as electrodes and lines, respectively. The proton conductivity was measured using a cell: copper|sample|copper. Measurements controlled by using an HDHWHS-50 incubator were taken in the temperature range of 25~80 °C with 95% relative humidity. ZSimpWin software was used to extrapolate impedance data results by means of an equivalent circuit simulation to complete the Niquist plot and obtain the resistance values.

The proton conductivity calculated as

$$\sigma = (1/R)\cdot(h/S)$$

where R is the resistance, h is the thickness, and S is the area of the disc.

Linear fitting of was used from the equation below:

$$\sigma T = \sigma_0 \exp(-Ea/k_B T)$$

where σ is the ionic conductivity, σ_0 is the preexponential factor, k_B is the Boltzmann constant, and T is the temperature.

Results and discussion

Synthesis and structural study

Compound **1** was synthesized at a relatively low reaction pH (~2.6). At this pH, the carboxylic acid groups are expected to be deprotonated, whereas the primary amine groups are protonated.

As shown in Fig. 1, the ionic crystal is composed of $[Al(OH)_6Mo_6O_{18}]^{3-}$ polyanions, $[Sm(H_2O)_5(CO_2CH_2NH_3)_2]^{3+}$ coordination cations and lattice water molecules. Sm^{3+} coordinates with five oxygen atoms from water molecules and four carboxyl O atoms from two glycine ligands with distorted tricapped trigonal prism coordination geometry. The polyoxometalates and macrocations lined up to form columns respectively by H-bonded interaction, which were alternately arranged in a honeycomb structure by electrostatic force (Fig. S8, ESI†). The distance between the oxygen atoms of the coordinated water molecules in the macrocations is 6.32 Å, and the oxygen atoms of the polyoxometalates in the adjacent column is 7.41 Å. The spaces between the columns were occupied with the lattice water molecules. Hence, the polyanions and the coordination cations stack to form a 3D supramolecular network structure containing 1D channels along c axis by electrostatic force and H-bonded interaction.

Significantly, 1D channels are lined exclusively by three of the five coordinated water molecules (H_2O15A, H_2O15B, H_2O17) of $[Sm(H_2O)_5(gly)_2]^{3+}$ forming hydrophilic inner surface with Anderson-type polyanions by H-bonded interaction. Besides, the crucial feature of **1** is the presence of repetitive array of water molecules in the 1D channels. Among five lattice water molecules (O1w–O5w) of the asymmetric unit of **1**, four (O2w–O5w) of them are involved in the formation of the water chains in 1D channels (Fig. 1 and Fig. S9, ESI†). In addition, structural analysis of **1** suggests the presence of protonated primary amines in $[Sm(H_2O)_5(gly)_2]^{3+}$.

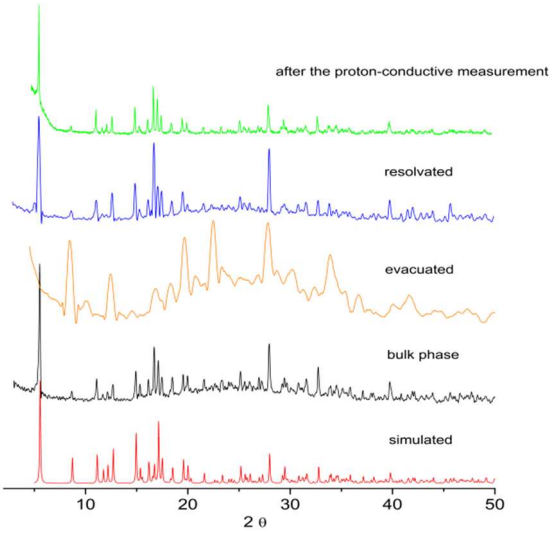

Fig. 2 Powder X-ray diffraction patterns of simulated **1** (red), as-synthesized **1** (black), dehydrated **1**, rehydrated **1** and **1** after proton conductive measurement (green).

Dynamic adsorption study

In General, ionic crystals based on POMs and macrocations possess unique guest sorption properties.[40-43] Thus, guest sorption property of **1** was investigated. Water sorption isotherm is present in Fig. S3 indicating that **1** can provide water uptake capacity of 6.15 wt%.

Thermogravimetric analysis revealed that loss of lattice waters occurred from room temperature to 97 °C (Fig. S2, ESI†). It suggests that repetitive array of water molecules in the 1D channels may be broken. However, the dehydrated samples (at 97 °C for 4 hours) exposed to 95% RH at 25 °C and 80 °C for 60 minutes were fully hydrated. It was confirmed powder X-ray diffraction (Fig. 2) and dynamic adsorption measurement (Fig. 3). Dynamic adsorption measurement was implemented at 1atm, 95% RH and representative temperatures (25 and 80 °C) using N_2 as carrier gas. As indicated in Figure 3, **1** showed a rapid adsorption process of water molecules in the initial 40 minutes and reached adsorption equilibrium within 60 minutes. The total water adsorption amount is 6.51 wt% (3.62 mmol g^{-1}) at 25 °C and 5.68 wt% (3.16 mmol g^{-1}) at 80 °C. This value is equivalent to approximate 6 water molecules per formula unit in accord with the number of lattice water molecules of **1** suggesting water chains still exist at elevated temperatures (80 °C) under 95% RH. Powder X-ray Diffraction (PXRD) results indicated the structure of dehydrated **1** is different from that of **1**, suggesting that framework of the ionic crystal may distort and even collapse in lack of guest molecules. However, PXRD spectra of rehydrated **1** is similar with that of simulated **1**, indicating rehydrated **1** maintained the same structure as the single-crystal as shown in PXRD results. This phenomenon can result from large electrostatic interaction between host–guest in that POMs possess electronegative oxygen atoms at the molecular surface.[40, 43]

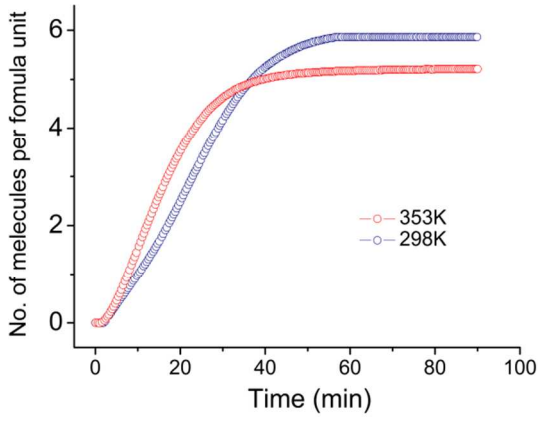

Fig. 3 Variation of H_2O uptake over time for **1** at 298 K (blue) and 353 K (red) under flowing N_2.

Proton Conductivity Study

Compound **1** possesses 1D channels with water molecules that interact with the coordinated water molecules and Anderson-type polyanion. These structural characteristics prompted us to investigate its proton conduction property. Then we measured water-assisted proton conduction in **1** which operates at low temperature (25~80 °C). AC impedance measurements of **1** were carried out using a two-probe method with Cu-pressed electrodes over the temperature range from 25 to 80 °C under 95% RH. The conductivities were determined from the Nyquist plots. Real (Z') and imaginary (Z'') parts of the impedance spectrum are shown in Fig. 4. The semi-circle in the high-frequency region corresponds to bulk and grain boundary resistance, whereas the tail at low frequency is consistent with mobile ions that are blocked by the electrode–electrolyte interface. The proton conductivity for **1** was found to be 4.85×10^{-6} S·cm^{-1} at 25 °C. The conductivity increases with increasing temperature and reaches 4.53×10^{-3} S·cm^{-1} upon the sample at 80 °C for 2 hours and subsequently water-equilibrated (Fig. 4). PXRD results indicated sample **1** maintained the same structure as the single-crystal before and after the proton-conductive measurements (Fig. 2).

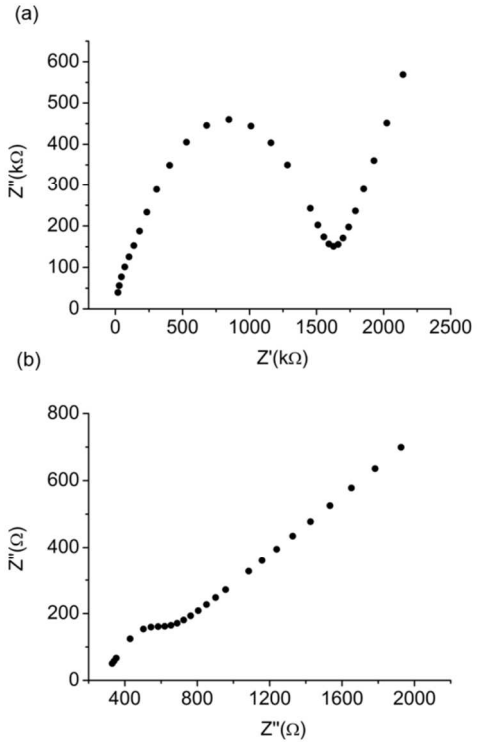

Fig. 4 Nyquist plots for **1** at 25°C (a) and 80°C (g) under 95% relative humidity.

To measure the conductivity of under varying humidity at 80 °C, impedance analyses were performed with different humidity in an incubator. Under 35% RH, the conductivity of **1** was found to be 3.17×10^{-6} S·cm^{-1}, which further increased slowly with increasing humidity, and under 65% RH, the conductivity increased to 1.46×10^{-5} S·cm^{-1}. The conductivity reaches a maximum value of 4.53×10^{-3} S·cm^{-1} under 95% RH. Dependence of the conductivity on humidity of **1** at 80 °C is present in Fig. 5 (a). The observed conductivity value of **1** at 80 °C under 95% RH is among the highest conductivity values that have been reported for POM-based ionic crystals under this relative humidity; it is higher than those of organic–inorganic

hybrid complexes based on POM, $\{[M(H_2O)_8][H(H_2O)_{2.5}](HINO)_4(PMo_{12}O_{40})\}_n$ (M = Co, Ni; HINO = isonicotinic acid N-oxide)[38] and $\{[Cu_3(L)_2(H_2O)_4][Cu(dmf)_4(SiW_{12}O_{40})]\cdot 9H_2O\}_n$ {L = N,N-bis[(2-hydroxy-3-methoxyphenyl)methylidene]hydrazine hydrate}[39] samples. Besides, it is comparable to those of ring-shaped organic–inorganic hybrid polyoxomolybdate, $[N(CH_3)_4]_{1.5}K_{5.5}Na_2[I_3\subset(Mo^{V}_2O_2S_2)_8(Se^{IV}O_3)_8(OH)_8]\cdot 25H_2O$[34] and $Na_5[H_7\{N(CH_2PO_3)_3\}Mo_6O_{16}(OH)(H_2O)_4]_4\cdot 18H_2O$[37]. In addition, we studied the time dependent proton conductivity of **1** at 80 °C under 95% RH for further application in fuel cells. Compound **1** showed similar proton conductivity even after 48 hours with a negligible loss of conductivity (Fig. 5 (b)). This result demonstrates the durability of the material for conduction, which is essential for practical applications.

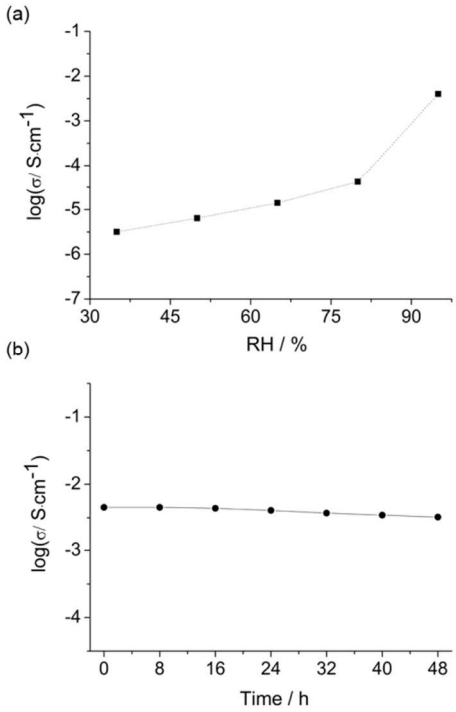

Fig. 5 (a) Dependence of the conductivity on humidity of **1** at 80 °C; (b) Time-dependent proton conductivity of **1** at 80 °C under 95% RH.

By preparing a similar compound using amine-free cations,[48] the proton conductivity of **1** was compared with the compound, $La(H_2O)_7[Al(OH)_6Mo_6O_{18}]\cdot 4H_2O$ ($La(H_2O)_7[AlMo_6]$) to confirm necessity of primary amine groups for proton conduction. The contrasting compound, $La(H_2O)_7[AlMo_6]$ consists of one-dimensional chains, built from alternating $[AlMo_6]^{3-}$ polyanions and $[La(H_2O)_7]^{3+}$ cations, and lattice water molecules, as shown in Fig. S10. There are extensive hydrogen bonds among surface of oxygen atoms of the Anderson-type polyanions, coordinated waters, and lattice water molecules (Fig. S10, ESI†). AC impedance measurement of $La(H_2O)_7[AlMo_6]$ was carried out from 25 to 80 °C under 95% RH. The result showed that conductivity value of **1** at 80 °C under 95% RH is higher than $La(H_2O)_7[AlMo_6]$ with conductivity of 1.7×10^{-6} S·cm^{-1}. It can be concluded that in this case the protonated primary amines play a vital role in high proton conductivity.

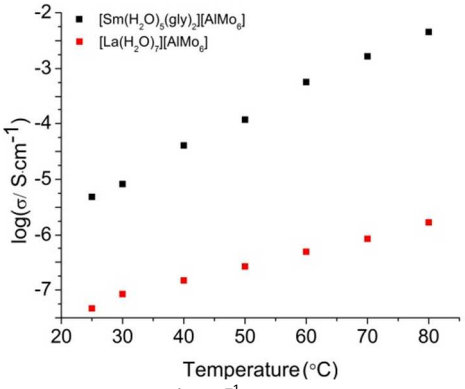

Fig. 6 Dependence of log(σ/S·cm^{-1}) on temperature under 98% RH for **1**(black) and $La(H_2O)_7[AlMo_6]$(red).

Two predominant mechanisms are widely accepted for proton conduction: Grotthuss mechanism and vehicle mechanism.[3, 12] The transport of protons between relatively stationary hosts is termed as Grotthuss mechanism, alternatively by other moveable species (OH^-, H_2O, H_3O^+, NH_4^+, HS^- etc.) is termed as vehicle mechanism.[49] Such processes have been identified primarily by activation energies obtained through Arrhenius plots. Generally, when the activation energy value of a material is greater than 0.6 eV, we can typically attribute it to vehicle transfer via water molecules.[50]

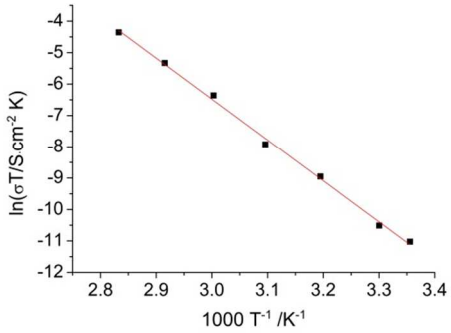

Fig. 7 Arrhenius plot of **1** showing the dependence of proton conductivity on temperature.

The activation energy of **1** calculated from Arrhenius plot of the proton conductivity is 1.09 eV (Fig. 7), which indicated that vehicle mechanism is typically attributed to protons transfer. The determined structure of **1** allows insight into proton transport mechanism: $[Sm(H_2O)_5(CO_2CH_2NH_3)_2]^{3+}$ coordination cations as Bronsted acid donate protons to water molecules which act as vehicles (H_3O^+, $H_5O_2^+$ etc.). Crystalline HPAs in many respects behave like solutions, designated by the term "pseudoliquid phase".[28, 29] In the circumstances, solid POMs behave like concentrated solutions of $H^+(H_2O)_n$, which

in the hydrophilic channels move along one definite direction, while lattice water molecules move along the opposite direction to complete proton transport. Thus, water chains exhibited in the channels can effectively transport protons dissociated from the protonated primary amines.

Conclusions

The hydrophilic environment of the 1D channels in as-prepared POM-based ionic crystal, created by the coordinated water molecules of macrocations and polyanions, provides stable proton transfer pathway; good proton conductivity was achieved above 10^{-3} $S \cdot cm^{-1}$ at 80 °C under 95% RH. Activation energy (Ea) for proton transfer in the **1** is 1.09 eV, typical of vehicle mechanism of proton conduction. High water content is retained when the starting sample exposed to 95% RH at 80 °C, although compound **1** is dehydrated at 97 °C or below. The proton conductivity of **1** was compared with a similar amine-free compound, indicating that the protons dissociated by the protonated primary amines play a vital role in high proton conductivity. Moreover, the crystallinity which enables molecular-level structure determination of **1** obtained by X-ray techniques allows insight into proton transport mechanism. As a consequence, POM-based inorganic-organic hybrids with water chains and additional protons will likely become an important class of proton conductive materials in the future.

Acknowledgements

This work was supported by the National Natural Science Foundation of China (Grants 21171032, 21371029 and 21231002), the Key Technologies R&D Program of Jilin Province of China (Grant 20130206079SF), and the Open Research Fund of the State Key Laboratory of Inorganic Synthesis and Preparative Chemistry (Jilin University, Grant 2015–01).

Notes and references

[a]*Key Lab of Polyoxometalate Science, Department of Chemistry, Northeast Normal University, Changchun 130024, PR China. E-mail: liusx@nenu.edu.cn; Fax: +86-431-85099328; Tel: +86-431-85099328*
[b]*School of Chemistry and Life Science, Changchun University of Technology, Changchun 130012, PR China.*
[c]*State Key Laboratory of Inorganic Synthesis and Preparative Chemistry, College of Chemistry, Jilin University, Changchun, 130012, PR China.*
[d]*Department of Chemistry, Zhejiang University, Hangzhou 310027, PR China.*

† Electronic Supplementary Information (ESI) available: Infrared analysis for **1** (Fig. S1). Thermogravimetric analysis for **1** (Fig. S2). Water adsorption and desorption isotherm for **1** (Fig. S3). Nyquist plots for **1** and the contrasting compound, $La(H_2O)_7[Al(OH)_6Mo_6O_{18}]\cdot 4H_2O$, (Fig. S4 and Fig. S5). Schematic representation of proton conduction for **1** (Fig. S6 and Fig. S7). Repetitive array of water molecules in 1D channels (Fig. S8). Crystal structure and hydrogen bonding interactions of the contrasting compound (Fig. S9) and additional supporting data. CCDC 967651 See DOI: 10.1039/b000000x/

1. S. M. Haile, D. A. Boysen, C. R. I. Chisholm and R. B. Merle, *Nature*, 2001, **410**, 910.
2. K. A. Mauritz and R. B. Moore, *Chem. Rev.*, 2004, **104**, 4535.
3. K.-D. Kreuer, S. J. Paddison, E. Spohr and M. Schuster, *Chem. Rev.*, 2004, **104**, 4637.
4. H. Zhang and P. K. Shen, *Chem. Rev.*, 2012, **112**, 2780.
5. G. K. H. Shimizu, J. M. Taylor and S. Kim, *Science*, 2013, **341**, 354.
6. S. Horike, D. Umeyama and S. Kitagawa, *Acc. Chem. Res.*, 2013, **46**, 2376.
7. M. Yoon, K. Suh, S. Natarajan and K. Kim, *Angew. Chem. Int. Ed.*, 2013, **52**, 2688.
8. T. Yamada, K. Otsubo, R. Makiura and H. Kitagawa, *Chem. Soc. Rev.*, 2013, **42**, 6655.
9. P. Ramaswamy, N. E. Wong and G. K. H. Shimizu, *Chem. Soc. Rev.*, 2014.
10. S. Bureekaew, S. Horike, M. Higuchi, M. Mizuno, T. Kawamura, D. Tanaka, N. Yanai and S. Kitagawa, *Nat Mater*, 2009, **8**, 831.
11. J. A. Hurd, R. Vaidhyanathan, V. Thangadurai, C. I. Ratcliffe, I. L. Moudrakovski and G. K. H. Shimizu, *Nat Chem*, 2009, **1**, 705.
12. T. Norby, *Solid State Ionics*, 1999, **125**, 1.
13. Y. Nagao, R. Ikeda, S. Kanda, Y. Kubozono and H. Kitagawa, *Molecular Crystals and Liquid Crystals*, 2002, **379**, 89.
14. H. Kitagawa, Y. Nagao, M. Fujishima, R. Ikeda and S. Kanda, *Inorg. Chem. Commun.*, 2003, **6**, 346.
15. S. S. Nagarkar, S. M. Unni, A. Sharma, S. Kurungot and S. K. Ghosh, *Angew. Chem. Int. Ed.*, 2014, **53**, 2638.
16. M. Bazaga-García, R. M. P. Colodrero, M. Papadaki, P. Garczarek, J. Zoń, P. Olivera-Pastor, E. R. Losilla, L. León-Reina, M. A. G. Aranda, D. Choquesillo-Lazarte, K. D. Demadis and A. Cabeza, *J. Am. Chem. Soc.*, 2014, **136**, 5731.
17. X. Meng, X.-Z. Song, S.-Y. Song, G.-C. Yang, M. Zhu, Z.-M. Hao, S.-N. Zhao and H.-J. Zhang, *Chem. Commun.*, 2013, **49**, 8483.
18. R. M. P. Colodrero, P. Olivera-Pastor, E. R. Losilla, M. A. G. Aranda, L. Leon-Reina, M. Papadaki, A. C. McKinlay, R. E. Morris, K. D. Demadis and A. Cabeza, *Dalton Trans.*, 2012, **41**, 4045.
19. M. Inukai, S. Horike, D. Umeyama, Y. Hijikata and S. Kitagawa, *Dalton Trans.*, 2012, **41**, 13261.
20. M. T. Pope and A. Müller, *Angewandte Chemie International Edition in English*, 1991, **30**, 34.
21. L. Cronin and A. Muller, *Chem. Soc. Rev.*, 2012, **41**, 7333.
22. H. N. Miras, J. Yan, D.-L. Long and L. Cronin, *Chem. Soc. Rev.*, 2012, **41**, 7403.
23. A. Banerjee, B. S. Bassil, G.-V. Roschenthaler and U. Kortz, *Chem. Soc. Rev.*, 2012, **41**, 7590.
24. H. Lv, Y. V. Geletii, C. Zhao, J. W. Vickers, G. Zhu, Z. Luo, J. Song, T. Lian, D. G. Musaev and C. L. Hill, *Chem. Soc. Rev.*, 2012, **41**, 7572.
25. J. T. Rhule, C. L. Hill, D. A. Judd and R. F. Schinazi, *Chem. Rev.*, 1998, **98**, 327.
26. J. M. Clemente-Juan, E. Coronado and A. Gaita-Arino, *Chem. Soc. Rev.*, 2012, **41**, 7464.
27. Y. Wang and I. A. Weinstock, *Chem. Soc. Rev.*, 2012, **41**, 7479.
28. I. V. Kozhevnikov, *Chem. Rev.*, 1998, **98**, 171.
29. N. Mizuno and M. Misono, *Chem. Rev.*, 1998, **98**, 199.

30. X. Tong, X. Wu, Q. Wu, W. Zhu, F. Cao and W. Yan, *Dalton Trans.*, 2012, **41**, 9893.
31. X. Qian, X. Tong, Q. Wu, Z. He, F. Cao and W. Yan, *Dalton Trans.*, 2012, **41**, 9897.
32. O. Nakamura, T. Kodama, I. Ogino and Y. Miyake, *Chem. Lett.*, 1979, **8**, 17.
33. Y. Zhou, J. Yang, H. Su, J. Zeng, S. P. Jiang and W. A. Goddard, *J. Am. Chem. Soc.*, 2014, **136**, 4954.
34. H.-Y. Zang, J.-J. Chen, D.-L. Long, L. Cronin and H. N. Miras, *Adv. Mater.*, 2013, **25**, 6245.
35. C. Dey, T. Kundu and R. Banerjee, *Chem. Commun.*, 2012, **48**, 266.
36. M. Wei, X. Wang and X. Duan, *Chemistry – A European Journal*, 2013, **19**, 1607.
37. L. Yang, P. Ma, Z. Zhou, J. Wang and J. Niu, *Inorg. Chem.*, 2013, **52**, 8285.
38. M.-L. Wei, P.-F. Zhuang, H.-H. Li and Y.-H. Yang, *Eur. J. Inorg. Chem.*, 2011, **2011**, 1473.
39. M.-L. Wei, J.-J. Sun and X.-Y. Duan, *Eur. J. Inorg. Chem.*, 2014, **2014**, 345.
40. S. Uchida and N. Mizuno, *Coord. Chem. Rev.*, 2007, **251**, 2537.
41. K. Suzuki, Y. Kikukawa, S. Uchida, H. Tokoro, K. Imoto, S.-i. Ohkoshi and N. Mizuno, *Angew. Chem. Int. Ed.*, 2012, **51**, 1597.
42. R. Eguchi, S. Uchida and N. Mizuno, *Angew. Chem. Int. Ed.*, 2012, **51**, 1635.
43. S. Uchida, R. Kawahara, Y. Ogasawara and N. Mizuno, *Dalton Trans.*, 2013, **42**, 16209.
44. M.-L. Wei, P.-F. Zhuang, Q.-X. Miao and Y. Wang, *J. Solid State Chem.*, 2011, **184**, 1472.
45. M.-L. Wei, P.-F. Zhuang, J.-H. Wang and X.-X. Wang, *J. Mol. Struct.*, 2011, **995**, 51.
46. M.-L. Wei, J.-H. Wang and Y.-X. Wang, *J. Solid State Chem.*, 2013, **198**, 323.
47. R. Cao, S. Liu, L. Xie, Y. Pan, J. Cao and Y. Liu, *Inorg. Chim. Acta*, 2008, **361**, 2013.
48. V. Shivaiah, P. V. Narasimha Reddy, L. Cronin and S. K. Das, *J. Chem. Soc., Dalton Trans.*, 2002, 3781.
49. X. Liang, F. Zhang, W. Feng, X. Zou, C. Zhao, H. Na, C. Liu, F. Sun and G. Zhu, *Chemical Science*, 2013, **4**, 983.
50. X. Liang, F. Zhang, H. Zhao, W. Ye, L. Long and G. Zhu, *Chem. Commun.*, 2014, **50**, 6513.

Graphical Abstract:

Proton conductive watery channels constructed by Anderson polyanions and lanthanide coordination cations

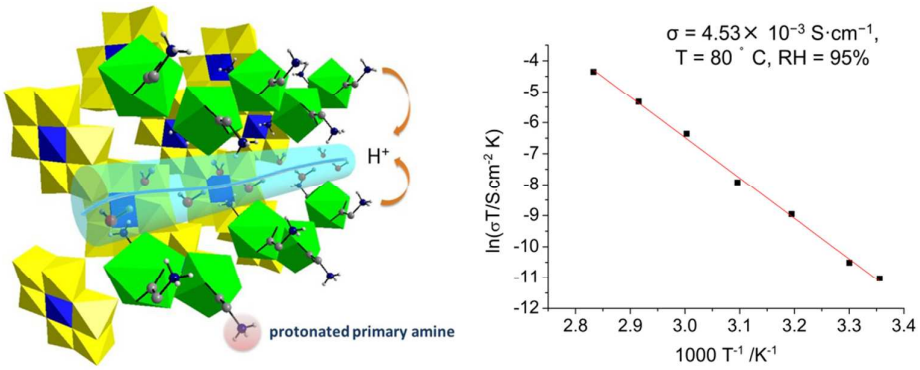

An ionic network based on Anderson POM featuring water chains in 1D channels exhibits outstanding proton conductivity.